

## Accepted Manuscript

Rheology of lignin-based chemical oleogels prepared using diisocyanate cross-linkers: effect of the diisocyanate and curing kinetics

A.M. Borrero-López, C. Valencia, J.M. Franco

PII: S0014-3057(16)31747-5

DOI: <http://dx.doi.org/10.1016/j.eurpolymj.2017.02.020>

Reference: EPJ 7722

To appear in: *European Polymer Journal*

Received Date: 23 December 2016

Revised Date: 13 February 2017

Accepted Date: 14 February 2017

Please cite this article as: Borrero-López, A.M., Valencia, C., Franco, J.M., Rheology of lignin-based chemical oleogels prepared using diisocyanate crosslinkers: effect of the diisocyanate and curing kinetics, *European Polymer Journal* (2017), doi: <http://dx.doi.org/10.1016/j.eurpolymj.2017.02.020>

This is a PDF file of an unedited manuscript that has been accepted for publication. As a service to our customers we are providing this early version of the manuscript. The manuscript will undergo copyediting, typesetting, and review of the resulting proof before it is published in its final form. Please note that during the production process errors may be discovered which could affect the content, and all legal disclaimers that apply to the journal pertain.



**Rheology of lignin-based chemical oleogels prepared using diisocyanate crosslinkers: effect of the diisocyanate and curing kinetics**

A.M. Borrero-López<sup>1</sup>, C. Valencia<sup>1,2</sup>, J.M. Franco<sup>1,2, ✉</sup>

<sup>1</sup>Departamento de Ingeniería Química. Campus de “El Carmen”. Universidad de Huelva. 21071 Huelva. Spain. Campus de Excelencia Internacional Agroalimentario, ceiA3.

<sup>2</sup>Pro<sup>2</sup>TecS – Chemical Product and Process Technology Center. Universidad de Huelva. 21071 Huelva. Spain.

✉ Author to whom correspondence should be addressed:

Prof. J.M. Franco. Departamento de Ingeniería Química, Química Física y Química Orgánica. Campus de “El Carmen”. Universidad de Huelva. 21071 Huelva. Spain.

Phone: +34959219995, Fax: +34959219983, e-mail: [franco@uhu.es](mailto:franco@uhu.es)

**Abstract**

In this work, alkali lignin together with different diisocyanates (hexamethylene diisocyanate (HDI), isophorone diisocyanate (IDI), toluene diisocyanate (TDI) and 4,4'-methylenebis (phenyl isocyanate) (MDI)) have been tested as gelling agents in a castor oil medium. A two-step process comprising first lignin functionalization with a diisocyanate and then the formation of a bio-based polyurethane with gel-like characteristics by combining the functionalized lignin with castor was followed. FTIR and thermogravimetry analysis were carried out on both the gelling agents and resulting oleogels. Moreover, oleogel rheological properties were evaluated by means of small-amplitude oscillatory shear (SAOS) tests and viscous flow measurements. The influences of time-temperature processing conditions during oleogel formation, lignin/diisocyanate ratio and functionalized lignin concentration on the rheological properties of oleogels were analyzed using HDI as crosslinker. 30% (w/w) thickener concentration and room temperature processing were selected to prepare oleogels with the rest of diisocyanates considered. Under the same conditions, HDI-functionalized lignin-based oleogels showed the strongest gel-like behavior whereas TDI-, IDI- and especially MDI-functionalized lignin-based oleogels displayed weak gel-like, or even a liquid-like, behaviors as a consequence of the respective chemical structures, which guide to higher steric hindrance, diminishing the formation of urethane linkages and/or Van der Waals forces. In general, oleogels exhibited an internal curing process due to the progressive formation of urethane linkages, which is closely related to the evolving rheological properties. The kinetics of this curing process was studied and an empirical model has been proposed to predict the evolution of the rheological properties with time.

**Keywords:** castor oil; diisocyanates; lignin; oleogel; rheology; urethanes

## 1. Introduction

In the last decades, the climate change and resources depletion have been increasing and changing the focus of research to more friendly environmental approaches. In that way, lignocellulosic materials are gaining more and more importance since they are renewable and ecological sources widespread around the world. Lignocellulosic materials include lignin, the second most abundant biopolymer after cellulose [1], which forms a random, amorphous three-dimensional network [2] and does not possess a well-defined structure but a complex combination among three main monomers (monolignols), i.e., p-hydroxyphenyl, guaiacyl and syringyl, and some others, as aliphatic hydroxyl groups, condensed phenol units, and carboxylic acid protons [3]. Paper industry is the main producer of lignin-rich residues, where around 98% are directly burned to recover energy. For these reasons, lignin is being focused as a promising material to obtain high-value added and environmental-friendly products.

In the same direction, several industries such as those involved in the production of lubricants [4–6] and adhesives [7] also face serious environmental problems [8] and are demanding eco-friendly oleogel-like systems with suitable functional properties, which can overcome these problems. Recently, some formulations which replace mineral or synthetic oils, in the case of lubricants [9–11], or volatile organic solvents, in the case of adhesives [12,13], by vegetable oils have been reported.

On the other hand, diisocyanates (HDI, IDI, TDI, MDI...) are capable of reacting with –OH groups of many polymers, e.g. butanediol polyester [14], hydroxyl-terminated polybutadiene and butacene [15], 4,4'-{oxy-1,4-diphenyl bis(nitromethylidene)}diphenol [16], glycidyl azide polymer [17], as well as graphene oxide [18] and mineral [19] and castor oils [20,21], to form urethane linkages (–NH–C(O)–O–) owing

to protons be transferred from  $-OH$  to the N in  $-NCO$  groups. These compounds are known to form materials with a wide variety of outstanding properties, depending on the application. In particular, some lignin-based polyurethanes have been already synthesized [1,22,23], even using castor oil as chain extender [24,25], thus adding the renewability and biodegradability characteristics sometimes desired for this type of materials. Similarly, HDI [11], TDI [13] and MDI [26,27] have demonstrated to be effective and efficient crosslinkers in oleogel formation and they can be used to chemically connect a vegetable oil and a suitable thickener agent. Among the different gelling agents in oil media, several isocyanate-functionalized cellulose and chitin derivatives have been previously proposed to form chemical gels in castor oil [28–30]. Considering the foregoing, this study is focused on combining lignin, as a well entangled, renewable, biodegradable and abundant material [31], with different diisocyanates as HDI, IDI, TDI and MDI as crosslinkers, to achieve a functionalized biopolymer which can be able to act as gelling agent in a castor oil (CO) medium. Following the methodology previously described for cellulose derivatives [32], in the present work a two-step oleogel formation which comprises firstly the lignin functionalization and secondly the formation of a chemical oleogel is proposed. This second step also involves chemical reactions, since free end-chain isocyanates, bonded to lignin or not, which had not already reacted can now react with the hydroxyl groups of the ricinoleic fatty acid chain. The main objective of this study was to investigate the influence of the type of diisocyanate crosslinker, the lignin/diisocyanate ratio, the NCO-functionalized lignin (FL) concentration and processing temperature on the rheological response of these chemical oleogels. Moreover, the kinetics of the chemical interaction between FL and CO, i.e., the curing process, was monitored by means of rheological measurements.

## 2. Experimental

### 2.1. Materials

Alkali lignin (L) obtained through a kraft process with up to 5% moisture and the different diisocyanates evaluated as crosslinkers, i.e. HDI, IDI, TDI and MDI, were purchased from Sigma-Aldrich. Purity of diisocyanate compounds was 98%, excepting for TDI (80%). Castor oil was purchased from Guinama (Spain). Fatty acid composition and main physical properties can be found elsewhere [33]. Other common reagents like toluene and triethylamine were analytical grade and also supplied by Sigma-Aldrich.

### 2.2. Functionalization reaction of lignin with diisocyanates

Lignin functionalization reaction was performed according to the methodology previously reported [32]. Briefly described, toluene (100 ml) was added to a round-bottom flask and maintained under argon inert atmosphere for 30 minutes. After that, a determined amount of lignin, followed by diisocyanate (in 1:1 and 1:2 lignin/diisocyanate weight ratios) and finally triethylamine (twice diisocyanate amount) were added and maintained for 24 hours under vigorous stirring at room temperature. The functionalized lignin (FL), purified under vacuum using a rotary evaporator, was prepared immediately before being used.

FLs were intended to be always prepared maintaining the same  $-OH/-NCO$  molar ratio for a given lignin/diisocyanate ratio. In this sense, a determined amount of lignin was mixed with the same amount of HDI for 1:1 ratio or double for 1:2 ratio. To maintain the same  $-OH/-NCO$  molar ratio for the rest of diisocyanates, the amount added for IDI-, TDI- and MDI-based FLs was calculated according to the different molecular weights:

$$IDI, TDI \text{ or } MDI = HDI \cdot \frac{MW_{IDI, TDI \text{ or } MDI}}{MW_{HDI}} \quad (1)$$

where HDI is the quantity of HDI that would be needed to add according to the above-mentioned lignin/diisocyanate ratio and  $M_w$ s are the molecular weights of the different diisocyanates. In the forthcoming text, for the sake of simplicity, the 1:1 and 1:2 lignin/diisocyanate ratio nomenclature will be maintained in all cases, assuming the correction of weights given by equation (1) for each diisocyanate. The different FLs were named with the codes included in Table 1 containing information of the lignin/diisocyanate ratio and type of crosslinker.

### 2.3. Preparation of oleogels

FL was mixed with castor oil in a stainless-steel reactor (100 mL) and generally maintained 24 hours under stirring at 70 rpm, using a controlled-rotational speed mixing device RW 20 (Ika), equipped with an anchor impeller. Processing of oleogels was generally carried out at room temperature, although the reaction was also accomplished at 70°C in order to study processing conditions. FL concentration was modified in the range of 20-30% (w/w) in the case of HDI-based FL. For the comparison of using different diisocyanates, a 30% (w/w) concentration was selected. Oleogels obtained were stored at room temperature and they will be referred using the codes included in Table 2.

### 2.4. Fourier Transform Infrared Spectroscopy (FTIR)

FTIR spectra were obtained using a JASCO FT/IR 4200 (Jasco inc. Japon). The gels, some FLs and all diisocyanates were characterized using KBr disks (32 x 3 mm), where the sample was placed between both disks. For lignin and solid FLs, KBr pellets

containing 10 parts of KBr and 1 part of sample were prepared by applying pressure for several minutes. In both cases, disks and pellets were placed in an adequate sample holder and FTIR were obtained between 400 and 4000  $\text{cm}^{-1}$ , at 4  $\text{cm}^{-1}$  resolution, in the transmission mode.

### **2.5. Thermogravimetric analysis (TGA)**

Measurements of mass loss with temperature was evaluated in the range from room temperature to 600°C, following a constant rise of 10°C/min, using a Q-50 model (TA Instrument Waters, USA) under N<sub>2</sub> purge. 5-10 mg of each sample were placed in a platinum pan previously tared and put onto the sample holder. After that, the measurement was automatically performed.

### **2.6. Rheological characterization.**

Linear viscoelasticity characterization of oleogels was carried out by means of SAOS tests in both the ARES (Rheometric Scientific) and the Rheoscope (Thermo Haake) rheometers, using roughened plate-plate geometries (25 and 20 mm, respectively, depending on the consistency of the sample, and 1 mm gap). Frequency sweep tests were performed inside the linear viscoelastic regime, in a frequency range of 0.03-100 rad/s. Strain or stress sweep tests were previously carried out to determine the linear viscoelastic range. Flow measurements were carried out in the ARES rheometer by applying an increasing stepped shear rate ramp from 0.01 to 100  $\text{s}^{-1}$ , taking 3 to 5 points each decade and maintaining the shear rate for three minutes in each step. Each rheological test was performed on fresh samples one week after oleogel formation and replicated at least twice. Moreover, in the case of oleogels prepared with HDI, a kinetic study was programmed, for which rheological measurements were performed from just 1 h after oleogel preparation up to one week.



### 3. Results and discussion

#### 3.1. Characterization of lignin and functionalized lignin samples

Lignin and functionalized lignin samples (FLs) were characterized using FTIR spectroscopy, as shown in Figure 1. Taking into account that spectra for all FLs are very similar, only results for the 1:1 lignin/HDI weight ratio functionalization is displayed. FTIR results confirm that new bonds were created in the functionalization process, yielding new and modified peaks in the spectra. Thus, a new peak appears at around  $3330\text{ cm}^{-1}$ , related to the N-H stretching vibration of new urethane bonds formed between -OH groups from lignin and -NCO from diisocyanates [32], and therefore the intensity of -OH stretching vibration band, centered at around  $3430\text{ cm}^{-1}$ , is significantly diminished, so that a sharper peak was found for FL in comparison with that obtained with non-functionalized lignin in the range of  $3300\text{-}3600\text{ cm}^{-1}$ . The two absorption bands around  $2934$  and  $2855\text{ cm}^{-1}$ , corresponding to asymmetric and symmetric C-H stretching vibration of aliphatic methylene groups are widely increased in FLs as a consequence of the new six-methylene chains in HDI moieties. Also, as intended, FLs exhibit a new intense peak centered at  $2270\text{ cm}^{-1}$ , corresponding to the stretching vibration of free isocyanate moieties. This peak is consequence of both, the free-one-side isocyanate bonded to lignin and possible non-reacted diisocyanates remained. Besides this, C=O bonds may generate two observable peaks in FTIR measurements, one related to C=O unconjugated bonds at around  $1710\text{ cm}^{-1}$  and the second related to C=O conjugated bonds, centered at around  $1620\text{ cm}^{-1}$  [34]. FLs spectra do not exhibit any clear signal corresponding to C=O unconjugated bonds but do show for C=O conjugated groups. Centered at around  $1570\text{ cm}^{-1}$ , another peak related to the urethane N-H bending vibration was observed only in FL IR spectrum, demonstrating once again the formation of urethane linkages.

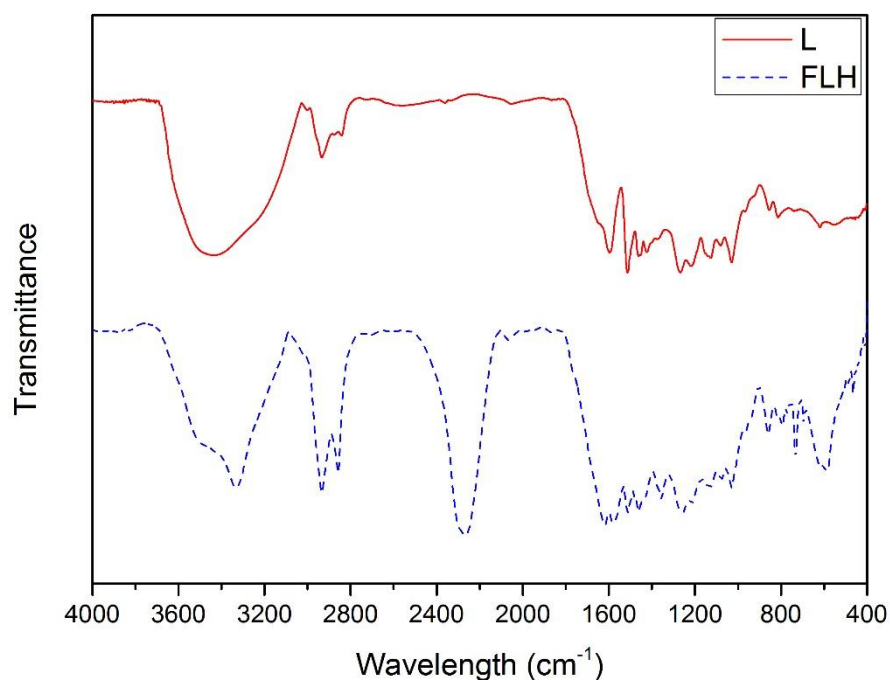


**Figure 1. Lignin and functionalized lignin FTIR spectra**

Thermogravimetric analyses were also used to characterize lignin and FL samples (Figure 2). Characteristic parameters considered for each thermal event were the onset temperature ( $T_{\text{onset}}$ ), temperature for the maximum weight loss rate ( $T_{\text{max}}$ ), final degradation temperature ( $T_{\text{final}}$ ) and weight loss ( $\Delta W$ ), whose values together with the final residue obtained at 600°C are shown in Table 1.

As can be seen, apart from the loss of moisture contained in the sample up to 100°C ( $\approx 3\%$ ) and the dehydration process of hydroxyl groups at around 165°C, lignin show one main weight loss peak at high temperatures with an associated  $T_{\text{max}}$  at 373°C (see Table 1), which according to the literature [35] may be attributed to the  $\beta$ -O-4 linkage breakdown, starting at around 250-300°C, the aliphatic side chains cleavage, starting at around 300°C, and disruption of C-C bonds among monolignols at around 400°C.

Moreover, the mass loss rate is very slow, yielding derivative weight loss not higher than 0.3 %/°C, which is in concordance with previous results [36].

Apart from the above mentioned mass loss events, properly related to the lignin-like structure, FLs thermograms also show another main degradation peak corresponding to the disruption of free –NCO segments, starting at around 100-140 °C [28]. This thermal event depends, however, on the type of diisocyanate compound employed to functionalize the lignin. For instance, attending to the results obtained for the 1:1 lignin/diisocyanate ratio, the temperature for the maximum degradation rate of –NCO segments is 119°C for HDI, whereas it is around 123-126°C for TDI and IDI, and 179°C for MDI. Similar tendency was observed for the 1:2 lignin/diisocyanate ratio. These degradation temperatures of –NCO segments in FL samples are roughly in agreement with those found in pure diisocyanates (Table 1).

Regarding the main mass loss detected in the non-functionalized lignin sample, the inclusion of diisocyanate compounds shifts the temperature for the maximum degradation rate to lower values. For instance, the lowest  $T_{max}$  value was observed for TDI-based FL sample obtained with 1:1 lignin/TDI ratio, followed by HDI-, MDI- and IDI-based FLs. Nevertheless, this difference is almost negligible for FL samples prepared with 1:2 lignin/diisocyanate ratio. Moreover, HDI-based FLs exhibit another peak at 437-454°C which was not detected in the raw lignin, which may be attributed to a high degree of crosslinking, as previously reported for other HDI-functionalized biopolymers [28]. On the other hand, FLs generate lower residue values in comparison with the non-functionalized lignin. HDI- and IDI-based FLs show lower residue values (around 19-24%) than TDI- and MDI-based FLs (35-40%).

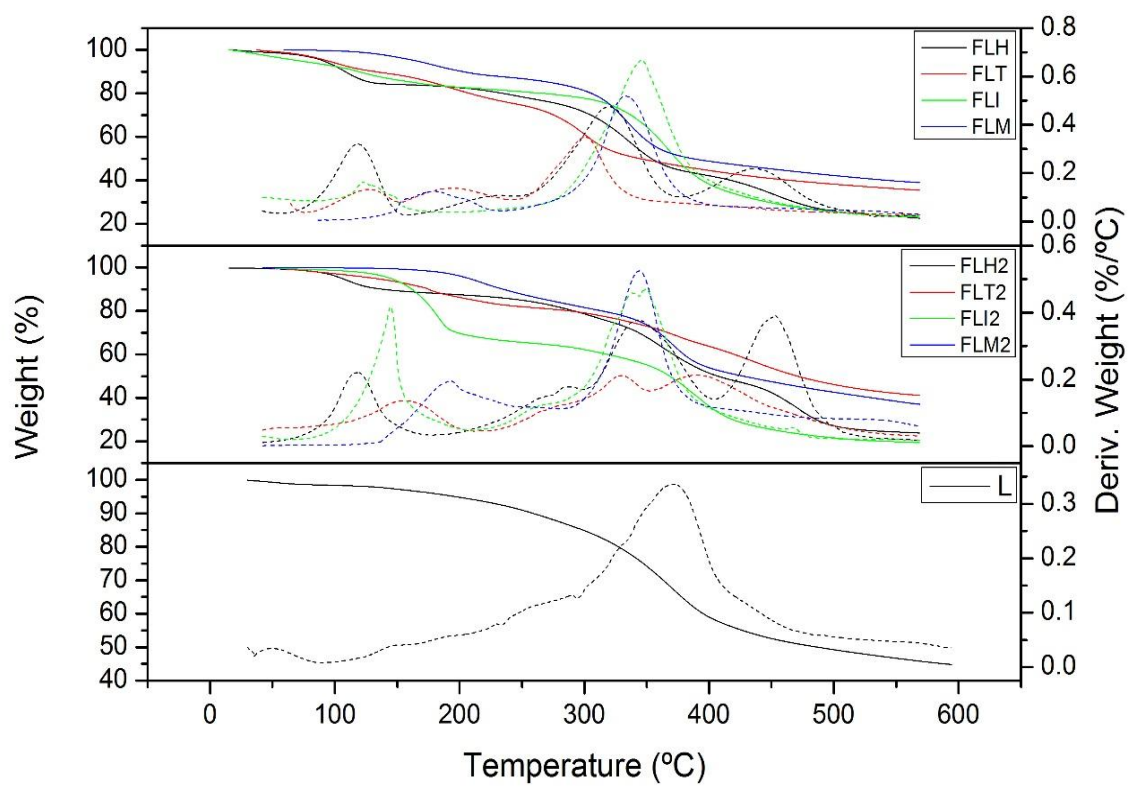


Figure 2. TGA curves for lignin and functionalized lignin samples

Table 1. TGA characteristic parameters of raw materials and functionalized lignin samples

Sample	Code	T <sub>onset</sub> (°C)	T <sub>max</sub> (°C)	T <sub>final</sub> (°C)	ΔW (%)	Residue (%)
Alkali lignin	L	27/129/249	61/164/373	92/183/407	3/4/49	44
HDI	HDI	137	172	178	99	1
TDI	TDI	116/172	155/181	159/188	84/14	2
IDI	IDI	124	177	184	100	0
MDI	MDI	174	221	227	97	3
L+HDI (1:1 ratio)	FLH	96/185/291/409	119/221/320/437	136/247/344/471.5	15/8/35/20	22
L+TDI (1:1 ratio)	FLT	102/171/275	126/195/300	143/216/322	11/17/37	35
L+IDI (1:1 ratio)	FLI	114/308	123/346	155/391	12/62	24
L+MDI (1:1 ratio)	FLM	121/303	179/333	205/361	14/46	40
L+HDI (1:2 ratio)	FLH2	98/298/429	118/344/454	134/375/475	11/41/24	24
L+TDI (1:2 ratio)	FLT2	144/266/371	160/331/391	178/341/443	16/19/25	40
L+IDI (1:2 ratio)	FLI2	100/245/318	153/261/355	174/286/393	33/8/40	19
L+MDI (1:2 ratio)	FLM2	162/321	192/345	233/363	18/47	35

### 3.2.Characterization of oleogels

#### 3.2.1. Influence of processing conditions

In order to optimize and gain a deeper knowledge on how processing conditions affect urethane bonds generation and therefore resulting oleogel rheological properties, the time and temperature, as two of the most important parameters during processing, are considered and modified. Two time-temperature conditions such as room temperature-

24 h (RT-24) and 70°C-3 hours (HT-3) were chosen as processing conditions, whereas the HDI-based FL with 1:1 lignin/HDI ratio, at 30% w/w concentration, was selected as chemical gelling agent to compare the different processes. FTIR spectra determinations were sequentially carried out after oleogel formation. As expected, a high processing temperature increases the reaction rate between free –NCO groups in FL and available –OH groups mainly located in the CO ricinoleic fatty acid chains, as can be seen in FTIR results in Figure 3a, where the spectra of just-obtained oleogels are shown. As can be seen, the NCO absorption band, at 2270  $\text{cm}^{-1}$ , almost disappear after 3 h at 70°C, whereas is clearly detectable after 24 h at room temperature. As well known, this residual amount of free –NCO groups still react after processing, which is called the curing process. However, despite the different kinetics during processing, as shown in Figure 3b, the curing time is extended up to 5-6 days, independently on the processing conditions, once free –NCO groups are not detected anymore. Nevertheless, processing conditions, i.e., time-T combination, dramatically influence oleogel rheological behavior after curing. As can be seen in Figure 4, a weak gel after curing was obtained by applying the HT-3 process, in contrast to that found when applying the RT-24 process conditions, which yields a strong gel response. This result may be explained taking into account that free isocyanates may react more randomly with different species, including themselves, at high temperatures [37], becoming other kind of linkages and limiting the chemical interaction between CO and FL, thus finally resulting much lower values of the storage ( $G'$ ) and loss ( $G''$ ) moduli (Figure 4a) and significantly higher values of the loss tangent ( $\tan \delta = G''/G'$ ) (Figure 4b).

Regarding the viscous flow response, a shear thinning behavior was always observed in the shear rate range studied, which may be fairly well described by the power-law model:

$$\eta = K \cdot \dot{\gamma}^{n-1} \quad (2)$$

where  $K$  and  $n$  are the consistency and flow indexes, respectively. After applying the HT-3 process conditions, lower viscosity values and higher flow index than those found in the oleogel processed with RT-24 conditions were obtained (see Figure 5 and power-law fitting parameters inset). Interestingly, in spite of all these differences found in the rheological behavior, TGA profiles (curves not shown) are almost identical for both types of oleogels (see relevant degradation temperatures in Table 2) and very similar to those reported for castor oil- and lignin-based flexible polyurethane foams [24], indicating that thermal degradation is mainly governed by FL and castor oil rather than the density and type of urethane linkages.

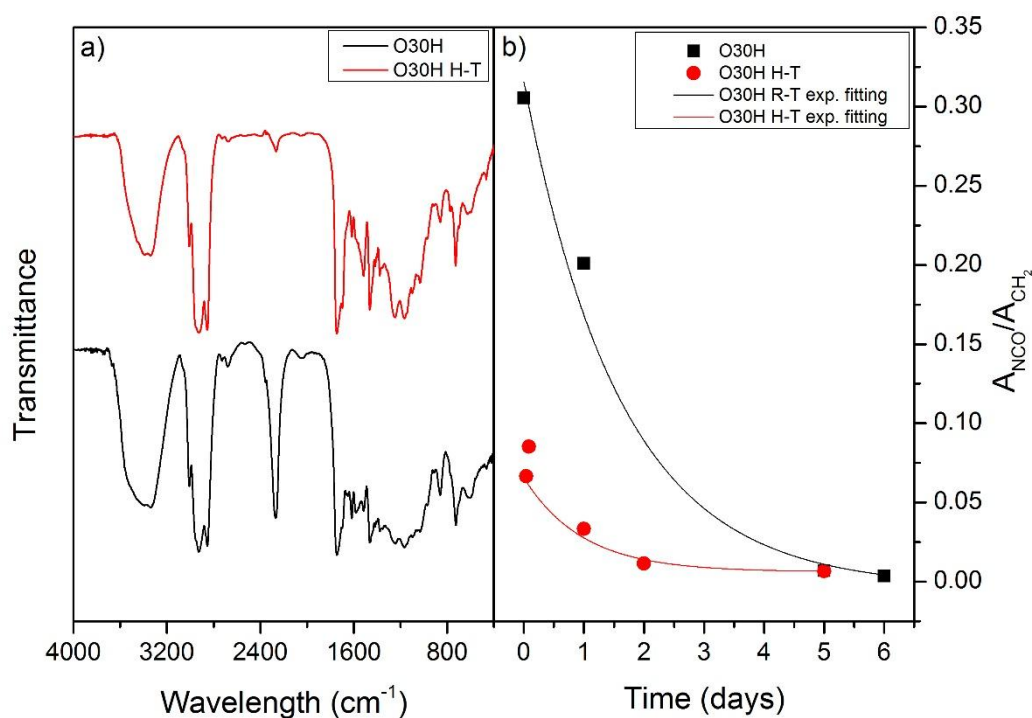


**Figure 3. a) FTIR spectra and b) evolution of isocyanate content with curing time for oleogels obtained applying different T-t processing conditions**

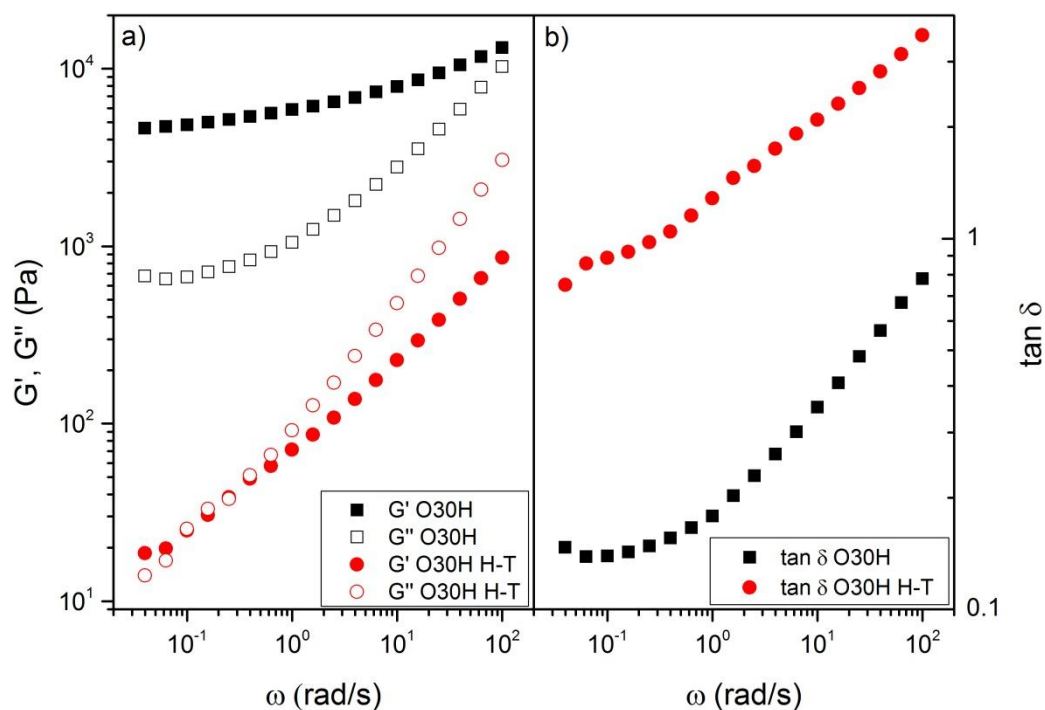


Figure 4. Evolution of a) the storage,  $G'$ , and loss,  $G''$ , moduli and b) the loss tangent,  $\tan \delta$ , with frequency for oleogels obtained applying different T-t processing conditions

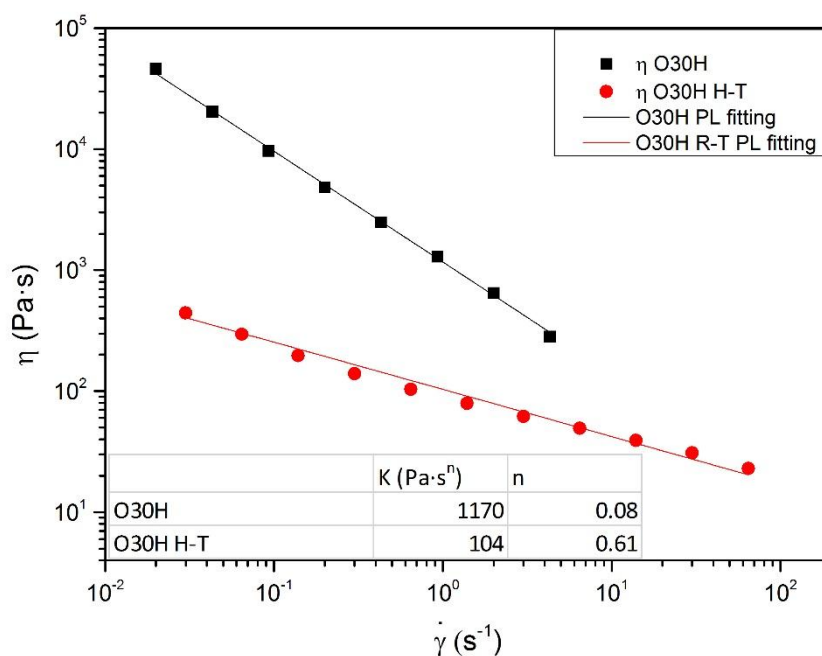


Figure 5. Viscous flow curves of oleogels obtained applying different T-t processing conditions. (Inside: power-law fitting parameters)



Table 2. TGA characteristic parameters of oleogel samples

Sample	Code	T <sub>onset</sub> (°C)	T <sub>max</sub> (°C)	T <sub>final</sub> (°C)	ΔW (%)	Residue (%)
Oleogel 30%FLH H-T	O30H H-T	335/427	378/439	427/459	82/10	8
Oleogel 20%FLH	O20H	337/422	382/431	297/457	80/16	4
Oleogel 25%FLH	O25H	334/420	381/442	398/463	84/11	5
Oleogel 30%FLH	O30H	324/425	379/439	397/458	83/11	6
Oleogel 30%FLT	O30T	275/355/423	311/380.5/446	334/397/454.5	16/64/15	5
Oleogel 30%FLI	O30I	290/360/427	327/382/450	332.5/398/459	22/59/17	2
Oleogel 30%FLM	O30M	286/358/437	320/378/441	330/398/463	16/69/11	4
Oleogel 20%FLH2	O20H2	304/366/423.5	334/382/451	339.5/398/456	23/60/17	0
Oleogel 25%FLH2	O25H2	306/362/432	333/384.5/447	350/403/465	24/59/13	4
Oleogel 30%FLH2	O30H2	301/358/431	343/381/445	358/408/466	28/53/12	7
Oleogel 30%FLT2	O30T2	282/355/425	311/380.5/439	320/396.5/463	21/61/11	7
Oleogel 30%FLI2	O30I2	296/357/417	327/379/424	329/395/446	29/46/17	8
Oleogel 30%FLM2	O30M2	285/361/433	320/386/454	328/404/473	19/67/13	1

### 3.2.2. Influence of functionalized lignin concentration and lignin/diisocyanate ratio

Oleogels containing different concentrations (20-30 % w/w) of HDI-based FL as gelling agent were prepared and the rheological response was analyzed. Figures 6 and 7 show the mechanical spectra obtained in the linear viscoelasticity regime and viscous flow curves, respectively, for oleogels containing 20, 25 and 30% w/w FL, and both 1:1 and 1:2 lignin/diisocyanate ratios. In general, both the SAOS functions and viscosity values

increase, around one order of magnitude, when using FL with 1:2 lignin/diisocyanate ratio in relation to the 1:1 ratio. This fact is simply explained attending the higher availability of free isocyanate moieties which guides to a higher degree of crosslinking between FL and CO. However, the SAOS functions frequency dependence is not qualitatively influenced by the lignin/diisocyanate ratio. On the other hand, as expected, for both 1:1 and 1:2 lignin/diisocyanate ratios, the higher the FL concentration, the higher the  $G'$ ,  $G''$  and viscosity values are. Moreover, 20% w/w oleogels show a crossover point between  $G'$  and  $G''$  at relatively high frequencies, as well as higher frequency dependence of SAOS functions (see Figure 6). This means a not well developed plateau region in the mechanical spectrum, which results in a shift of the transition region to lower frequencies, according to the typical behavior of not highly entangled gel networks [38]. A more extended plateau region with a crossover point shifted to higher frequencies was observed by increasing FL concentration. This effect was dampened by modifying the lignin/diisocyanate ratio from 1:1 to 1:2, since the degree of crosslinking is higher, as above mentioned.

Viscosity values depend on FL concentration in the same way as  $G'$  and  $G''$  do. Nevertheless, similar viscosity values, especially at high shear rates, were obtained for oleogels containing 25 and 30% w/w FL using the 1:2 lignin/HDI ratio. Table 3 collects the values of the power-law fitting parameters. As can be observed,  $K$  values increase with FL concentration and decrease with lignin/HDI ratio, whereas extremely low values of the flow index were generally observed, which is the consequence of the typical yielding behavior found in gel-like dispersions [39–41]. Only the oleogel prepared with 20% w/w FL and 1:1 lignin/HDI weight ratio shows a different flow behavior with an exceptionally high value of the flow index, as a result of a not so extensively crosslinked-network achieved at this concentration (see also Figure 6).

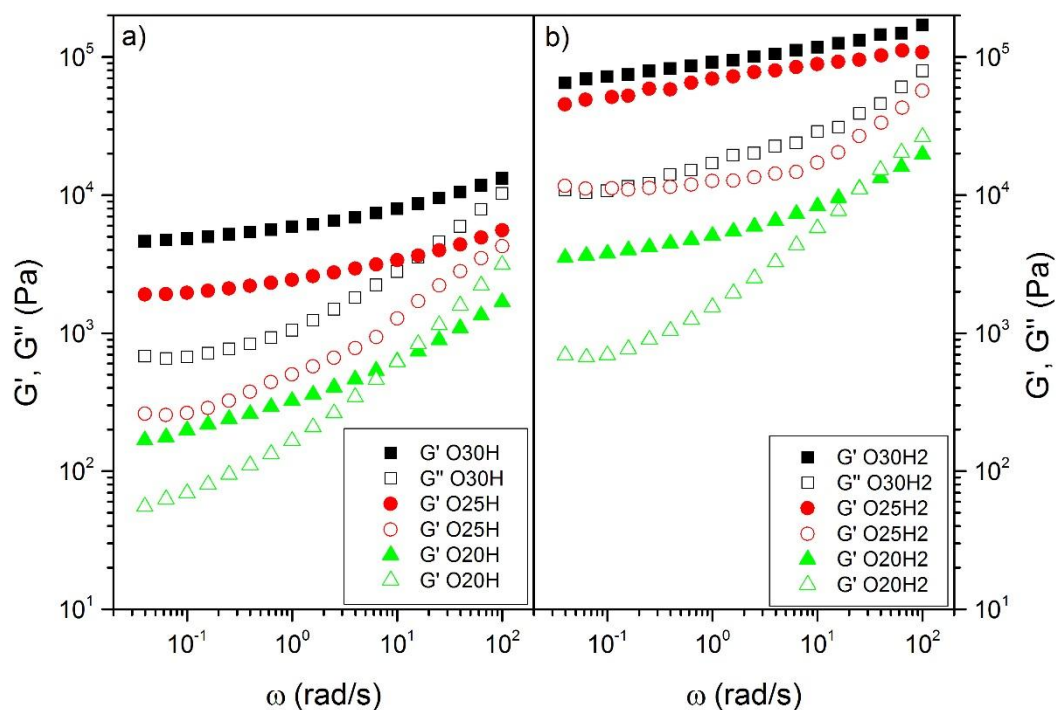


**Figure 6.** Frequency dependence of SAOS functions for HDI-FL-based oleogels as a function of FL concentration (a) 1:1 lignin/HDI ratio, b) 1:2 lignin/HDI ratio)

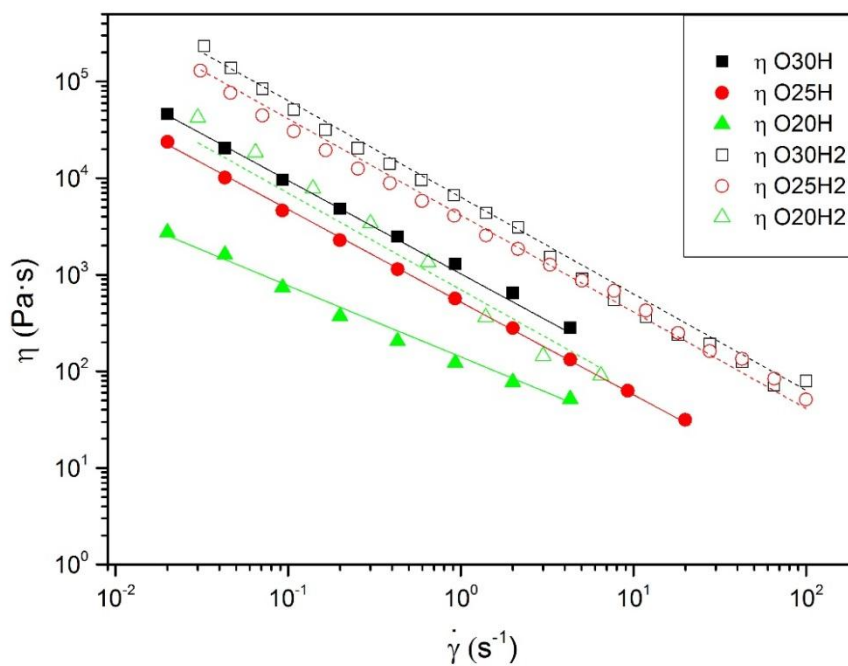


**Figure 7.** Viscous flow curves for HDI-FL-based oleogels as a function of FL concentration and lignin/HDI ratio

**Table 3. K and n values for HDI, IDI, TDI and MDI-FL-based oleogels**

Samples	K (Pa·s <sup>n</sup> )	n
O30H	1170	0.08
O25H	522	0.04
O20H	141	0.26
O30H2	6343	0.01
O25H2	4120	0.01
O20H2	70	0.01
O30T	126	0.60
O30I	89	0.94
O30M	14	0.91
O30I2	48375	0.86
O30M2	52	0.93

Despite the large influence on the rheological response, FL concentration and lignin/diisocyanate ratio do not significantly affect FTIR and TGA profiles of oleogels. Since the rheological characterization was carried out just after curing (one week after processing), it is logical that FTIR spectra of all oleogels were very similar, since chemical composition is essentially the same in that moment. Regarding TGA profiles, most remarkable effect is the disappearance of the first degradation peak, corresponding to free isocyanate groups, found in FL samples (see Figure 2), corroborating the almost complete reaction of these groups after one week of curing. Moreover, all the oleogels show a main degradation stage with  $T_{\max}$  at around 379-384°C, although the temperature range is broadened in those prepared with FLs having 1:2 lignin/diisocyanate ratio (see  $T_{\text{onset}}$  and  $T_{\text{final}}$  values in Table 2), as previously found in NCO-functionalized methylcellulose-based oleogels [28].

### 3.2.3. Influence of the type of diisocyanate used as crosslinker

The comparison of the rheological response of oleogels prepared with different types of diisocyanates was carried out for 30% w/w FL concentration and both 1:1 and 1:2 lignin/diisocyanate ratios. Chemical structure of different diisocyanates, i.e.,

conformational shape, bonds and molecular size, is one of the main factors determining the rheological behavior of resulting oleogels. Briefly described, HDI contains a small linear chain between both isocyanate groups, while the other three compounds are cyclic. TDI is an aromatic ring with isocyanates in positions 2 and 4, IDI is a cyclic hexane with three methylene groups joined and free isocyanates disposed in positions 1 and 3 and, finally, MDI is composed of two-phenyl rings joined by a methylene group and diisocyanates symmetrically disposed in *para* position respect to the methylene group. However, despite the different chemical structures, urethane bonds generated are similar and therefore oleogel FTIR spectra are analogous, although the evolution of isocyanate content with curing time is different, as will be discussed more in deep in next section.

On the other hand, regarding TGA results, for completely cured oleogels, again the first peak observed in FLs was not detected. Only one main peak centered on CO decomposition, at around 379-386°C, with small shoulders at both sides, is evidenced in all gels (see characteristic temperatures in Table 2). Temperature ranges for these overlapped degradation peaks are similar for all oleogels and comprise thermal degradation of both CO and FL, also considering the chemical interaction between both of them. IDI-FL-based oleogels show the highest loss in both shoulders, increasing as the lignin/diisocyanate ratio increases, and the smallest peak in maximum weight loss, decreasing from 1:1 to 1:2 ratio (see Table 2).

More dramatical differences were found in the rheological responses. The evolutions of SAOS functions with frequency are compared in Figure 8, as a function of the type of diisocyanate employed. Oleogel containing FL with 1:2 lignin/TDI ratio was not included since a rather heterogeneous sample was obtained, probably due to an excessive crosslinking degree achieved during lignin functionalization. However, as can

be observed, TDI-FL-based oleogel, for 1:1 lignin/TDI ratio, shows a weak gel-like behavior, response quite close to a critical gel [42], with similar values of  $G'$  and  $G''$ . This weak gel-like behavior may be explained attending the size, rigidity and, therefore steric hindrance of TDI molecule, much higher than HDI, which favors lower crosslinking density. This effect is even emphasized when using IDI and MDI as crosslinkers, resulting not really gels but liquid-like viscoelastic dispersions. In the case of the systems containing 1:2 lignin/IDI ratio, however, a tendency to reach a crossover point between  $G'$  and  $G''$  was observed at high frequencies. This rheological response is probably related with a higher difficulty when bonding and also with lower Van der Waals forces because of IDI chemical structure [14]. Supporting this, MDI, with the greater steric hindrance, yields the lower values of  $G'$  and  $G''$ , being  $G'' \gg G'$  in the whole frequency range studied, even for the 1:2 lignin/MDI ratio.

Viscous flow measurements shown in Figure 9 also reflect huge differences among the oleogels prepared with different diisocyanates. In general, much lower viscosity values, several orders of magnitude, and smoother shear-thinning behavior were found when using TDI, IDI and especially MDI as crosslinkers, in comparison to HDI-FL-based oleogels (see power-law parameters in Table 3). For IDI and MDI, again similar responses were displayed, both oleogels exhibiting an almost completely Newtonian behavior. Following the same tendency than that previously discussed for SAOS results, IDI-FL-based oleogel viscosity is higher than those obtained for MDI-FL-based ones, around one order of magnitude higher for the 1:1 lignin/diisocyanate ratio. Interestingly, FL containing 1:2 lignin/IDI ratio, provides an oleogel with exceptionally high and almost constant viscosity values, even higher than those obtained for HDI-FL-based oleogels. This extremely high viscosity values are in agreement with the high  $G''$  values obtained at high frequencies in SAOS tests. Finally, an intermediate response was

obtained with TDI-FL-based oleogel, exhibiting generally higher viscosity values, but also a lower flow index, than oleogels prepared with MDI- and IDI-based FL.

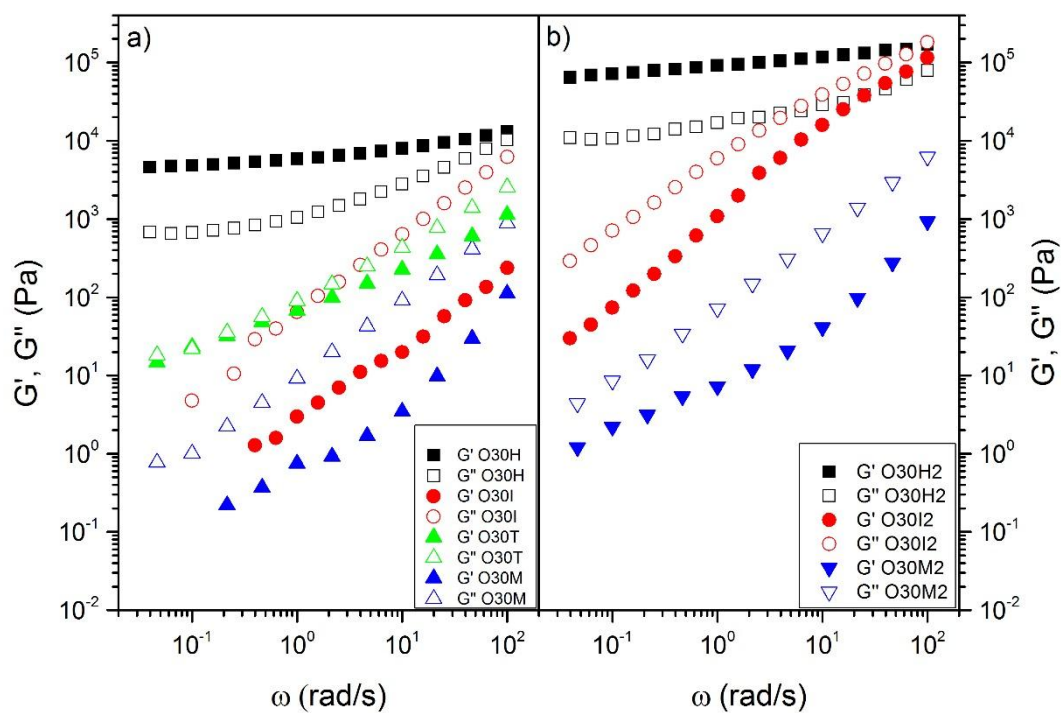


**Figure 8.** Frequency dependence of SAOS functions for oleogels prepared with different types of diisocyanates (a) 1:1 lignin/ diisocyanate ratio, b) 1:2 lignin/ diisocyanate ratio)

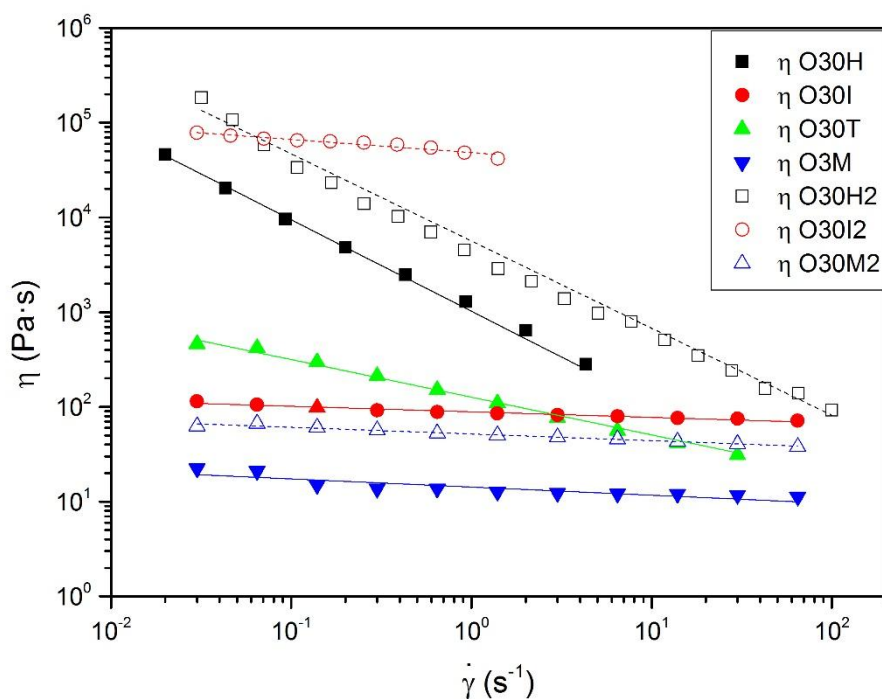


**Figure 9. Viscous flow curves of oleogels prepared with different types of diisocyanates**

### 3.2.4. Curing kinetics

As explained above, FL-based oleogels undergo an internal process of curing. However, this curing process does not follow the same kinetics for the different diisocyanates considered. As can be observed in Figure 10, the progressive disappearance of free –NCO during curing, monitored through the evolution of the –NCO intensity band in FTIR spectra, is totally different for each of the diisocyanates employed as crosslinkers. Since areas of the different bands are correlated with the concentration of functional groups in a given sample, the decrease in intensity of the isocyanate peak with curing time is a real representation of isocyanate loss by chemical reactions in the sample. As peak intensity and area depend on the quantity of sample added to the KBr plate or pellet, as well as surface exposed, changes in peak values may be due not only to



isocyanate reaction inside the sample. To remove that negative effect, the area of the characteristic isocyanate band at  $2270\text{ cm}^{-1}$  was considered relative to the areas of  $\text{CH}_2$  groups at  $2934$  and  $2855\text{ cm}^{-1}$ , which are constant for an oleogel along the whole curing process, being the evolution of isocyanate content with time considered proportional to  $A_{\text{NCO}}/A_{\text{CH}_2}$  [22]. HDI-FL-based oleogels show an exponential decay of free  $-\text{NCO}$  content with curing time, till 6-12 days after preparation when the residual free  $-\text{NCO}$  content is negligible. Similar trend was observed in IDI-FL-based oleogels, although the initial isocyanate content is higher and the kinetics much slower, achieving the total loss of  $-\text{NCO}$  groups during the second week or even longer in the case of the 1:2 lignin/IDI ratio. On the contrary, TDI-FL-based oleogels exhibited a quick decay of free  $-\text{NCO}$  content, no longer than 3-4 days, which unexpectedly does not completely disappear but remain constant at a significant level. More surprising is the behavior found in MDI-FL-based oleogels, where no decay was observed at all, being the free  $-\text{NCO}$  content equal, or even slightly higher, to that obtained just after oleogel preparation. This means that the curing process does not occur in fact, which explains the liquid-like rheological response obtained.

Therefore, the relationship between the loss of free  $-\text{NCO}$  groups during curing and the final oleogel rheological properties seems to be closely related. Moreover, the evolution of isocyanate content also modifies the rheological properties along the curing process. Since HDI-FL-based oleogels achieved stronger gel-like characteristics, these systems have been selected at a 25% w/w FL concentration and both 1:1 and 1:2 lignin/HDI weight ratios to study more in deep the kinetics of the curing process from a rheological point of view. Figure 11 displays a detailed evolution of  $A_{\text{NCO}}/A_{\text{CH}_2}$  with time for the two HDI-FL-based oleogels selected, showing the expected initial higher values for the oleogel prepared with FL containing 1:2 lignin/HDI ratio respect to the 1:1 ratio, as well

as the exponential decay of values with curing. At the same time, SAOS measurements were performed equitably separated three times the same day of oleogel preparation, twice the following day and once per day until 1 week. Figure 12 displays the evolution of SAOS functions with frequency for the oleogel prepared with the 1:2 lignin/HDI weight ratio FL sample and selected curing times, from 2h to one week after preparation. As can be observed, the values of the storage and loss moduli increase with curing time predominantly during the first 24h (Figure 12a), which is in agreement with the evolution of free  $-NCO$  groups shown in Figure 11. Moreover, the loss tangent (Figure 12b) significantly decreases during these first stages of the curing process, especially at high frequencies, and remains almost constant after 24h, also exhibiting a minimum which is shifted to higher frequencies with the progress of curing, as a consequence of the achievement of a more expanded plateau region. Measurements after one and two months were also performed to gain further insight at much longer times after completion of the curing process, roughly providing the same results than those reported for one week (data not shown).

As the plateau region of the mechanical spectrum, more or less extended, was always detected for HDI-based oleogels, the plateau modulus,  $G_N^0$ , the characteristic parameter of this region in the mechanical spectrum, which can be straightforwardly estimated as [43]:

$$G_N^o = [G']_{\tan \delta \rightarrow \text{minimum}} \quad (3)$$

has been selected to analyze and model the curing kinetics. Moreover, since the loss tangent is not substantially affected by the curing process after 24h, the whole SAOS mechanical spectrum may be determined from  $G_N^0$  values. Figure 13 shows the evolution of the normalized plateau modulus, being  $G_{N-0}^0$  and  $G_{N-\infty}^0$  the values of the

plateau modulus at time zero after oleogel preparation, and for the totally cured oleogel, respectively. For the HDI-FL-based oleogel containing 1:1 lignin/HDI ratio, a rather fast increase in the values of SAOS functions was obtained during the first day after processing, achieving a maximum value at around 20-30 h of ageing, still remaining approximately 25-30% of the initial free isocyanate content. However, unexpectedly, once this maximum value was reached,  $G'$  and  $G''$  values decreased for the following two days and finally a slight increase was observed after one week, remaining constant further on, as illustrated in Figure 13. This evolution may be explained considering two contrary effects, on one hand the strengthening of the oleogel sample as the crosslinking degree increases through the formation of new urethane bonds chemically bonding FL and CO, and on the other hand, the relaxation of the gel network as a consequence of the non-physical equilibrium during the progress of the chemical reaction [44]. During the first hours, chemical reaction kinetics has much more importance on the rheology than any relaxation process, as free  $-NCO$  groups concentration is still high (see Figure 11). However, after one day, available free  $-NCO$  groups have significantly diminished its concentration, and relaxation of the oleogel network gains more importance in detriment of the effect of crosslinking formation. Finally, the equilibrium is achieved once isocyanate content was negligible. On the other hand, the oleogel containing a 1:2 lignin/HDI ratio exhibits a different behavior. Even when both mentioned processes come about at the same time, isocyanate concentration is much higher than for the 1:1 lignin/HDI ratio, resulting a more extensively crosslinked network which dampens structural relaxation. Thus, the values of the SAOS moduli progressively increase after oleogel preparation, achieving the maximum value at longer times, approximately coinciding with the equilibrium, as a consequence of the higher amount of residual free  $-NCO$  groups, which obviously need more time to react completely (see Figure 11).

The evolution of the plateau modulus with the curing time has been modeled for oleogels containing 25% w/w FLH and FLH2, i.e., 1:1 and 1:2 FL/HDI ratios, using a modified consecutive-reaction kinetic equation:

$$\frac{G_N^0 - G_{N-0}^0}{G_{N-\infty}^0 - G_{N-0}^0} = \left( B \cdot t \cdot \frac{k_1}{k_2 - k_1} - 1 \right) \cdot (A \cdot e^{-k_1 \cdot t} - (A - 1) \cdot e^{-k_2 \cdot t}) + 1 \quad (4)$$

which takes into account both internal processes during curing, i.e., the strengthening according to isocyanate loss through the kinetic constant  $k_1$  and structural relaxation through constant  $k_2$ , where  $A$  and  $B$  are fitting parameters considering the relative weight of both exponential terms and the absolute values of the normalized plateau modulus, respectively. As shown in Figure 13, reasonable good fittings were obtained in both cases (see fitting parameters in Table 4).

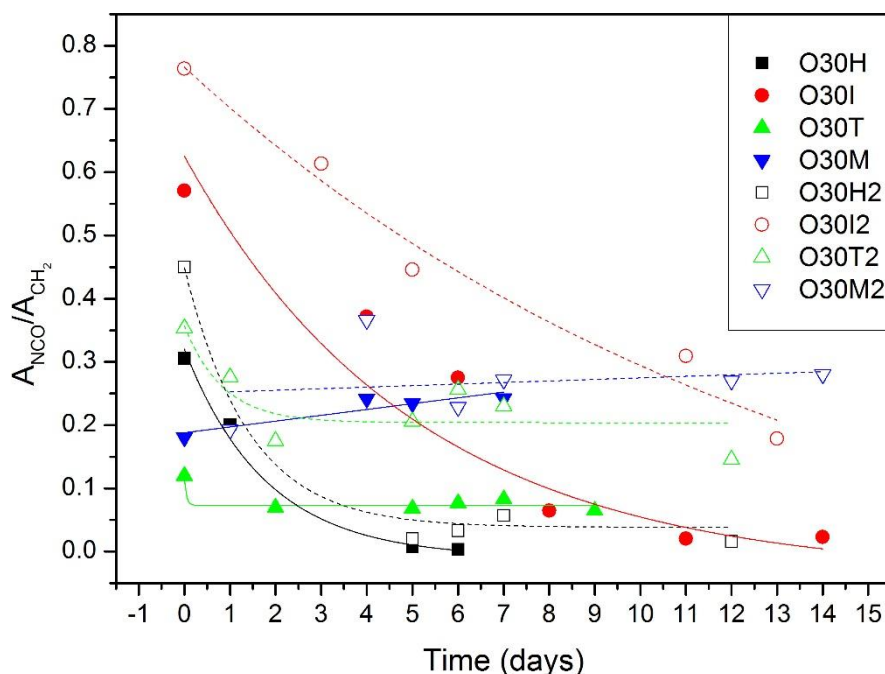


**Figure 10.** Evolution of free isocyanate content with curing time for oleogels prepared with different types of diisocyanates

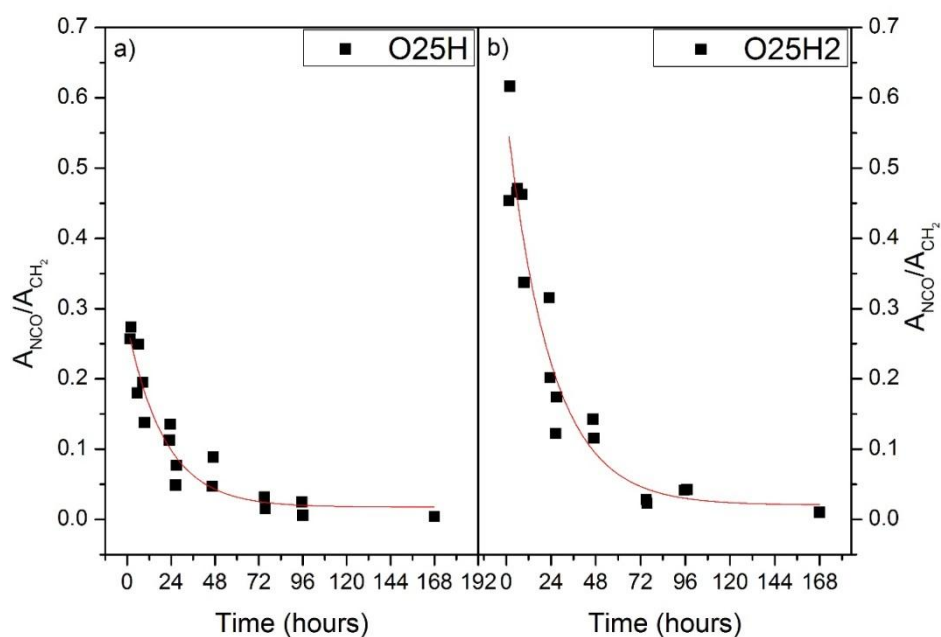


Figure 11. Evolution of free isocyanate content with curing time for 25% HDI-FL-based oleogels (a) 1:1 lignin/ diisocyanate ratio, b) 1:2 lignin/ diisocyanate ratio)

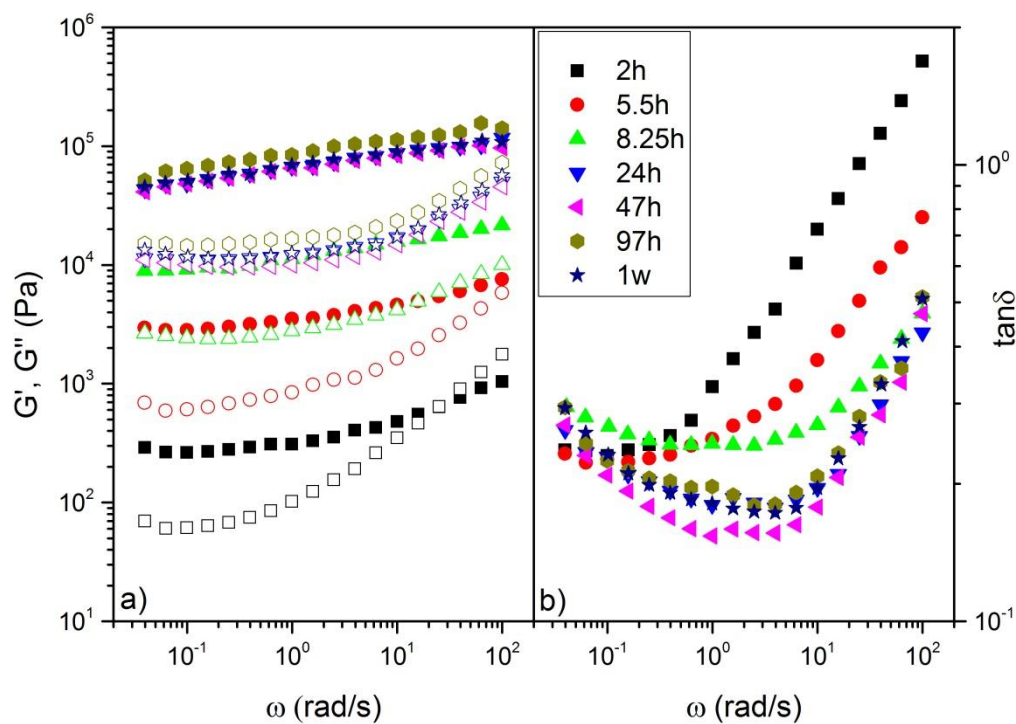
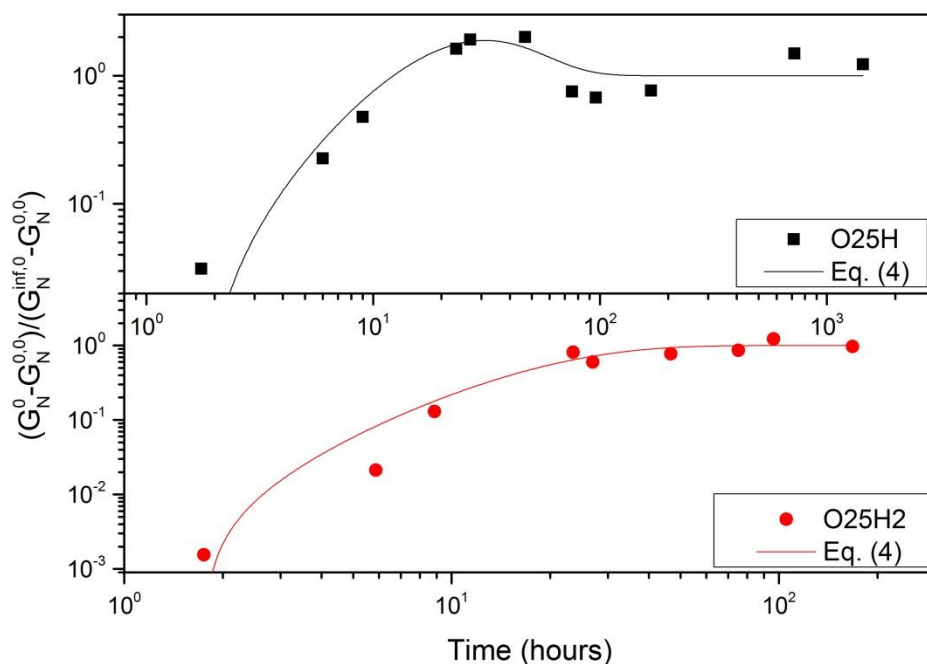


Figure 12. Evolution of SAOS functions with curing time for O25H2 sample



**Figure 13.** Evolution of the normalized plateau modulus with curing time and fitting to equation (4)

**Table 4.** Equation (4) fitting parameters for oleogels containing 25% w/w FLH and FLH2

Sample	$G_{N-0}^0$ (Pa)	$G_{N-\infty}^0$ (Pa)	$B$ ( $h^{-1}$ )	$A$	$k_1$ ( $h^{-1}$ )	$k_2$ ( $h^{-1}$ )	$R^2$
1:1	21	4015	8.0 E-4	250	0.0805	0.0813	0.83
1:2	65	80379	7.4 E-4	3	0.0953	0.0946	0.92

#### 4. Conclusions

Lignin, a promising renewable and residual polymeric material in the paper industry, has been successfully tested, along with diisocyanate crosslinkers, as gelling agent in a castor oil medium by applying a two-step oleogel preparation protocol which comprises firstly the lignin functionalization and secondly the formation of bio-based

polyurethanes with gel-like characteristics by combining the functionalized lignin with castor oil. Time-temperature processing conditions influence oleogel formation and related rheological properties. A high processing temperature (70°C) shortens oleogel preparation by accelerating the formation of new urethane linkages between the functionalized lignin and castor oil, but however yields a weak gel-like response. Oleogel rheological properties can be modulated by modifying the functionalized lignin concentration or the lignin/diisocyanate ratio in the functionalization reaction, thus varying the crosslinking density afterwards.

The chemical structure of the diisocyanate compound used as crosslinker dramatically influences oleogel rheological properties. Thus, IDI and especially MDI produce liquid-like viscoelastic dispersions, in contrast to the strong gel-like characteristics found in HDI-based oleogels, whereas an intermediate response was observed for TDI-based oleogels.

The evolution of free isocyanate content during curing, i.e., after oleogel preparation, is also influenced by the type of diisocyanate, showing an exponential decay for HDI and IDI, and small variation for TDI and MDI. The kinetics of this curing process has been analyzed from a rheological point of view and explained as two different processes occurring simultaneously, the strengthening of the samples by the formation of new urethane linkages and the gel network structural relaxation. A modified consecutive-reaction kinetic model has been proposed to describe the evolution of the plateau modulus with curing time.

## 5. Acknowledgments

This work is a part of two research projects (CTQ2014-56038- C3-1R and TEP-1499) sponsored by the MINECO-FEDER and Junta de Andalucía programmes, respectively.

## 6. Bibliography

- [1] H. Jeong, J. Park, S. Kim, J. Lee, N. Ahn, H. Gyoo Roh, Preparation and characterization of thermoplastic polyurethanes using partially acetylated kraft lignin, *Fibers Polym.* 14 (2013) 1082–1093. doi:10.1007/s12221-013-1082-7.
- [2] M. Chávez Sifontes, M.E. Domine, Lignina, estructura y aplicaciones: métodos de despolimerización para la obtención de derivados aromáticos de interés industrial, *Avances en Ciencias e Ingeniería.* 4 (2013) 15–46. doi:http://www.exeeedu.com/publishing.cl/av\_cienc\_ing/2013/Vol4/Nro4/3-ACI1184-13-full.pdf.
- [3] C.A. Cateto, Lignins as Macromonomers for Polyurethane Synthesis: A Comparative Study on Hydroxyl Group Determination, *Polym. Polym. Compos.* 21 (2013) 449–456. doi:10.1002/app.
- [4] C.W. Lea, European development of lubricants derived from renewable resources, *Ind. Lubr. Tribol.* 54 (2002) 268–274. doi:10.1108/00368790210445632.
- [5] B. Wilson, Lubricants and functional fluids from renewable sources, *Ind. Lubr. Tribol.* 50 (1998) 6–15. doi:10.1108/00368799810781274.
- [6] J.E. Martín-Alfonso, C. Valencia, M.C. Sánchez, J.M. Franco, C. Gallegos, Development of new lubricating grease formulations using recycled LDPE as rheology modifier additive, *Eur. Polym. J.* 43 (2007). doi:10.1016/j.eurpolymj.2006.09.020.
- [7] D.E.Á. Packham, *International Journal of Adhesion & Adhesives Adhesive technology and sustainability*, 29 (2009) 248–252. doi:10.1016/j.ijadhadh.2008.06.002.
- [8] J.O. Metzger, M. Eissen, Concepts on the contribution of chemistry to a sustainable development . *Renewable raw materials*, 7 (2004) 569–581. doi:10.1016/j.crci.2003.12.003.
- [9] R. Sánchez, C. Valencia, J.M. Franco, Rheological and Tribological Characterization of a New Acylated Chitosan–Based Biodegradable Lubricating Grease: A Comparative Study with Traditional Lithium and Calcium Greases, *Tribol. Trans.* 57 (2014) 445–454. doi:10.1080/10402004.2014.880541.
- [10] L.A. García-Zapateiro, C. Valencia, J.M. Franco, Formulation of lubricating greases from renewable basestocks and thickener agents: A rheological approach, *Ind. Crops Prod.* 54 (2014) 115–121. doi:10.1016/j.indcrop.2014.01.020.
- [11] R. Gallego, J.F. Arteaga, C. Valencia, M.J. Diaz, J.M. Franco, Gel-Like Dispersions of HMDI-Cross-Linked Lignocellulosic Materials in Castor Oil: Toward Completely Renewable Lubricating Grease Formulations, *ACS Sustain. Chem. Eng.* 3 (2015) 2130–2141. doi:10.1021/acssuschemeng.5b00389.
- [12] K.P. Somani, S.S. Kansara, N.K. Patel, A.K. Rakshit, Castor oil based polyurethane adhesives for wood-to-wood bonding, *23* (2003) 269–275. doi:10.1016/S0143-7496(03)00044-7.



- [13] B.B.R. Silva, R.M.C. Santana, M.M.C. Forte, International Journal of Adhesion & Adhesives A solventless castor oil-based PU adhesive for wood and foam substrates, *Int. J. Adhes. Adhes.* 30 (2010) 559–565. doi:10.1016/j.ijadhadh.2010.07.001.
- [14] M. V. Pandya, D.D. Deshpande, D.G. Hundiwale, Effect of diisocyanate structure on viscoelastic, thermal, mechanical and electrical properties of cast polyurethanes, *J. Appl. Polym. Sci.* 32 (1986) 4959–4969. doi:10.1002/app.1986.070320518.
- [15] B. Lucio, J.L. De La Fuente, M.L. Cerrada, Characterization of Phase Structures of Novel Metallo-Polyurethanes, *Macromol. Chem. Phys.* 216 (2015) 2048–2060. doi:10.1002/macp.201500238.
- [16] D.P. Suhas, H.M. Jeong, T.M. Aminabhavi, A. V. Raghu, Preparation and characterization of novel polyurethanes containing 4,4'-{oxy-1,4-diphenyl bis(nitromethylidene)}diphenol schiff base diol, *Polym. Eng. Sci.* 54 (2014) 24–32. doi:10.1002/pen.23532.
- [17] Z.J. Zhang, Y.J. Luo, G.P. Li, Reaction kinetics of GAP and three kinds of isocyanates with variable temperature FTIR spectrum method, 22 (2014) 382–385. doi:10.3969/j.issn.1006-9941.2014.03.020.
- [18] U. Saha, R. Jaiswal, J.P. Singh, T.H. Goswami, Diisocyanate modified graphene oxide network structure: Steric effect of diisocyanates on bimolecular cross-linking degree, *J. Nanoparticle Res.* 16 (2014). doi:10.1007/s11051-014-2404-4.
- [19] G. Moreno, C. Valencia, J.M. Franco, C. Gallegos, A. Diogo, J.C.M. Bordado, Influence of molecular weight and free NCO content on the rheological properties of lithium lubricating greases modified with NCO-terminated prepolymers, *Eur. Polym. J.* 44 (2008). doi:10.1016/j.eurpolymj.2008.04.047.
- [20] A.A. Cuadri, F.J. Navarro, P. Partal, Isocyanate-functionalized castor oil as a novel bitumen modifier, *Chem. Eng. Sci.* 97 (2013) 320–327. doi:10.1016/j.ces.2013.04.045.
- [21] A.A. Cuadri, M. García-Morales, F.J. Navarro, P. Partal, Effect of transesterification degree and post-treatment on the in-service performance of NCO-functionalized vegetable oil bituminous products, *Chem. Eng. Sci.* 111 (2014) 126–134. doi:10.1016/j.ces.2014.02.028.
- [22] C.A. Cateto, M.F. Barreiro, A.E. Rodrigues, Monitoring of lignin-based polyurethane synthesis by FTIR-ATR, *Ind. Crops Prod.* 27 (2008) 168–174. doi:10.1016/j.indcrop.2007.07.018.
- [23] A. Arshanitsa, L. Krumina, G. Telysheva, T. Dizhbite, Exploring the application potential of incompletely soluble organosolv lignin as a macromonomer for polyurethane synthesis, *Ind. Crop. Prod.* 92 (2016) 1–12. doi:10.1016/j.indcrop.2016.07.050.
- [24] J. Bernardini, P. Cinelli, I. Anguillesi, M.B. Coltelli, A. Lazzeri, Flexible polyurethane foams green production employing lignin or oxypropylated lignin, *Eur. Polym. J.* 64 (2015) 147–156. doi:10.1016/j.eurpolymj.2014.11.039.
- [25] L.B. Tavares, C. V. Boas, G.R. Schleder, A.M. Nacas, D.S. Rosa, D.J. Santos, Bio-based polyurethane prepared from Kraft lignin and modified castor oil, *Express Polym. Lett.* 10 (2016) 927–940. doi:10.3144/expresspolymlett.2016.86.
- [26] D. Wolfgang Schröder, W. Klaus Jenni, Crosslinked castor oil derivatives, US

- Patent 5 387 658 (1995).
- [27] M.M. Jin, Y.J. Luo, Preparation and characterization of nitrocellulose aerogel, 36 (2013) 82–86.
- [28] R. Gallego, J.F. Arteaga, C. Valencia, J.M. Franco, Rheology and thermal degradation of isocyanate-functionalized methyl cellulose-based oleogels, *Carbohydr. Polym.* 98 (2013) 152–160. doi:10.1016/j.carbpol.2013.04.104.
- [29] R. Gallego, M. González, J.F. Arteaga, C. Valencia, J.M. Franco, Influence of functionalization degree on the rheological properties of isocyanate-functionalized chitin- and chitosan-based chemical oleogels for lubricant applications, *Polymers* 6 (2014) 1929–1947. doi:10.3390/polym6071929.
- [30] R. Gallego, J.F. Arteaga, C. Valencia, J.M. Franco, Thickening properties of several NCO-functionalized cellulose derivatives in castor oil, *Chem. Eng. Sci.* 134 (2015) 260–268. doi:10.1016/j.ces.2015.05.007.
- [31] J. Zakzeski, P.C.A. Bruijninx, A.L. Jongerius, B.M. Weckhuysen, The Catalytic Valorization of Lignin for the Production of Renewable Chemicals, (2010) 3552–3599.
- [32] R. Gallego, J.F. Arteaga, C. Valencia, J.M. Franco, Chemical modification of methyl cellulose with HMDI to modulate the thickening properties in castor oil, *Cellulose*. 20 (2013) 495–507. doi:10.1007/s10570-012-9803-4.
- [33] L.A. Quinchia, M.A. Delgado, C. Valencia, J.M. Franco, C. Gallegos, Viscosity modification of different vegetable oils with EVA copolymer for lubricant applications, *Ind. Crops Prod.* 32 (2010) 607–612. doi:10.1016/j.indcrop.2010.07.011.
- [34] K.K. Pandey, A study of chemical structure of soft and hardwood and wood polymers by FTIR spectrscopy, *J. Appl. Polym. Sci.* 71 (1999) 1969–1975. doi:10.1002/(sici)1097-4628(19990321)71:12<1969::aid-app6>3.3.co;2-4.
- [35] C. Liu, H. Wang, A.M. Karim, J. Sun, Y. Wang, Catalytic fast pyrolysis of lignocellulosic biomass, *Chem. Soc. Rev.* 43 (2014) 7594–7623. doi:10.1039/C3CS60414D.
- [36] H. Yang, R. Yan, H. Chen, D.H. Lee, C. Zheng, Characteristics of hemicellulose, cellulose and lignin pyrolysis, *Fuel.* 86 (2007) 1781–1788. doi:10.1016/j.fuel.2006.12.013.
- [37] S. Velankar, S.L. Cooper, Microphase Separation and Rheological Properties of Polyurethane Melts. 1. Effect of Block Length, *Macromolecules.* 31 (1998) 9181–9192. doi:10.1021/ma9811472.
- [38] C. Liu, J. He, E. Van Ruymbeke, R. Keunings, C. Bailly, Evaluation of different methods for the determination of the plateau modulus and the entanglement molecular weight, 47 (2006) 4461–4479. doi:10.1016/j.polymer.2006.04.054.
- [39] P. Coussot, Q.D. Nguyen, H.T. Huynh, D. Bonn, Avalanche Behavior in Yield Stress Fluids, *Phys. Rev. Lett.* 88 (2002) 175501. doi:10.1103/PhysRevLett.88.175501.
- [40] M.A. Delgado, C. Valencia, M.C. Sánchez, J.M. Franco, C. Gallegos, Thermorheological behaviour of a lithium lubricating grease, *Tribol. Lett.* 23 (2006) 47–54. doi:10.1007/s11249-006-9109-5.
- [41] G. Ovarlez, S. Cohen-addad, K. Krishan, J. Goyon, P. Coussot, *Journal of Non-*

- Newtonian Fluid Mechanics On the existence of a simple yield stress fluid behavior, *J. Nonnewton. Fluid Mech.* 193 (2013) 68–79. doi:10.1016/j.jnnfm.2012.06.009.
- [42] L. Lu, X. Liu, Z. Tong, Critical exponents for sol-gel transition in aqueous alginate solutions induced by cupric cations, *Carbohydr. Polym.* 65 (2006) 544–551. doi:10.1016/j.carbpol.2006.02.010.
- [43] J.E. Martín-Alfonso, J.M. Franco, Influence of polymer reprocessing cycles on the microstructure and rheological behavior of polypropylene / mineral oil oleogels, *Polym. Test.* 45 (2015) 12–19. doi:10.1016/j.polymertesting.2015.04.016.
- [44] M. Dandapat, D. Mandal, *Spectrochimica Acta Part A : Molecular and Biomolecular Spectroscopy* Local viscosity and solvent relaxation experienced by rod-like fluorophores in AOT / 4-chlorophenol / m-xylene organogels, *SAA.* 170 (2017) 150–156. doi:10.1016/j.saa.2016.07.012.

## HIGHLIGHTS

- NCO-functionalized lignin as chemical gelling agent of castor oil
- Rheological properties of chemical oleogels dramatically depend on the type of diisocyanate used as crosslinker
- Oleogel rheological properties can be modulated by modifying the functionalized lignin concentration and the lignin/diisocyanate ratio
- A modified consecutive-reaction kinetic model describes the evolution of viscoelastic modulus with curing time

ACCEPTED MANUSCRIPT